ANALYSIS OF SPILLS USING AN AIRBORNE LASER FLUOROSENSOR

D. Diebel, T. Hengstermann, R. Reuter
Universität Oldenburg
Fachbereich Physik
D-2900 Oldenburg, FRG

SUMMARY

Airborne fluorosensor measurements over oil spills were performed during ARCHIMEDES 2 in the German Bight, and in the "MARPOL Exercise" in Dutch waters. It is shown that the fluorosensor method enables a sensitive detection of small volumes of pollutants which give rise to surface films having a thickness in the order of 1 µm. The results give also evidence of the complicated behaviour of oil dispersed at sea due to the influence of wind and waves. In particular, it is the balance of clear water and oil fluorescence contributions and its spectral variability from which information can be derived.

Parts of the findings are not yet well understood. In addition to temporal changes in the optical characteristics of the mineral oil itself, surface active substances being components of the oil seem to be responsible for certain variations of the optical signature in the edge areas of slicks where films with sub-micrometre thickness are present.

INTRODUCTION

It has been demonstrated in the remote sensing experiment ARCHIMEDES I using the Oceanographic Lidar System (OLS) that the application of fluorescence techniques from airborne platforms provides information on the presence, composition and film thickness of mineral oil on the sea surface [Diebel-Langohr et al., 1985].

Data obtained over heavy fuel oil and chocolate mousse spills revealed that it is in particular the balance of fluorescence from the mineral oil and from naturally occurring organic matter (Gelbstoff) dissolved in the water column which allows an evaluation of the oil type and of the alterations of its optical properties after spilling. Film thickness measurements ranging between 0.1 and 10 µm have been obtained from analyzing the suppression of water Raman scattering due to absorption of laser light and of Raman scattered light within the strongly absorbing surface film.

To further investigate the capabilities of the airborne fluorosensor method, and to obtain data from oil types other than heavy fuel, ARCHIMEDES 2 has been carried out as a subsequent experiment in the German Bight northwest of Helgoland in October 1985. In this campaign, successful application of OLS was hampered by unfavorable weather conditions with very poor visibility in the test area, and by a defective Omega navigation system of the research aircraft Do 28. Due to these circumstances, only the spilled Ekofisk crude oil ("spill A") could be investigated.

It was therefore decided to perform another experiment. For specific examination of the

capabilities of the airborne fluorosensor, the experiment focussed on detecting and analyzing small volumes of mineral oil typically occurring following controlled discharges by ship traffic. This experiment, the "MARPOL Exercise", was performed off the Dutch coast in May 1986 and in cooperation with Rijkswaterstaat.

PRINCIPLE OF OPERATION

The hydrographic laser fluorosensor consists of a high power pulse laser and of a telescope receiver for the detection of laser-induced radiation from the upper layers of the sea. Laser excitation is generally chosen in the near UV or at blue wavelengths, where water shows good transparency and where fluorescence of dissolved and suspended substances (e.g. Gelbstoff, plankton) can be efficiently excited. Characteristic fluorescence spetra of these substances and the Raman scatter of water reveal distinct peaks covering the whole visible spectrum above the laser wavelength. From a specific registration of these spectral signatures, the concentration of fluorescent matter and the light attenuation coefficient can be evaluated [Hoge and Swift, 1983a; Bristow et al., 1985; Reuter et al. 1986].

In the presence of an oil spill, signals originating from the water column are damped due to absorption of light within the oil film. Since the absorption coefficient of crude oils and heavy refined products is of the order of 1 μm^{-1} at UV and blue wavelengths, water column signals are completely obscured by films having more than a few micrometer thickness.

Complementary to this damping process, characteristic fluorescence of mineral oils is excited. Their fluorescence spectra cover the entire visible spectrum above the laser wavelength. Optically thick surface films yield an intensity comparable to that produced by natural seawater compounds in turbid coastal areas [Diebel-Langohr et al., 1985].

Registration of the shape of the spectrum provides a mean to estimate the oil type: with UV excitation, light oils are characterized by strong fluorescence at blue wavelengths, the fluorescence yield of heavy oils being markedly reduced and showing maximum values in the green part of the spectrum [e.g. Thruston and Knight, 1971; Kung and Itzkan, 1975; Visser, 1979; O'Neil et al., 1980; Diebel-Langohr et al., 1985].

Measurements of the thickness of oil films require an estimation of the oil specific absorption coefficient since signal dynamics are governed by exponentials, $\exp -((c_1+c_d)_o * d)$, with $(c_1 + c_d)_o$ the sum of absorption coefficients of the mineral oil at the laser and the detection wavelength, respectively, and d the thickness of the surface film. With the availability of signature catalogs of optical properties of mineral oils [e.g. Hoge, 1982; Schwarz, 1982; Hengstermann, 1987] which include both absorption and fluorescence data, absorption coefficients can be estimated from the measured fluorescence spetra. Film thickness of surface spills is then derived from the depression of Raman scatter from the water column [Kung and Itzkan, 1975; Hoge and Swift, 1980] or from the increase in oil fluorescence intensity [Visser, 1979; Hoge, 1983].

The theory of the measuring process is based on the lidar equation [Browell, 1977], and on its integration over arbitrary layers on the water surface or in the water column. This integral and the evaluation of algorithms for fluorosensor data interpretation are described in detail in Diebel-Langohr et al., 1985.

An optically thin layer on the water surface with a film thickness d results in a detector signal

$$P_{o,w} \sim \sigma_o/\alpha_o + (\sigma_w/\alpha_w - \sigma_o/\alpha_o) * \exp(-\alpha_o * d)$$

with σ_o and σ_w the fluorescence efficiency of the mineral oil and the water column (for the latter including also Raman scatter contributions to the measured signal intensity), α_o and α_w the sum of attenuation coefficients at the laser and the detector wavelength $\alpha_{o/w} = (c_1 + c_d)_{o/w}$ of the oil and the water, respectively.

Measurements of the thickness d of the film are preferably done using the water Raman scattering which in the case of an oil-free water surface provides an intensive and well defined spectral peak occurring at 344 nm with an excitation at 308 nm. However, problems exist due to the underlying fluorescence background at the water Raman scatter wavelength arising from Gelbstoff and mineral oil. To overcome this problem, the water Raman scatter intensity R is estimated by extrapolating a baseline using fluorescence intensities measured at neighbouring detection channels (in this case at 366 and 380 nm, see below). This procedure necessitates accurate calibration of the spectral sensitivities of the detection channels used for the extrapolation.

Normalization of the calculated water Raman scatter intensity R_w obtained over the oil-free water column to the calculated values $R_{o,w}$ measured over the oil film yields

$$R_{o,w}/R_w = \exp(-\alpha_o * d).$$

A solution for the film thickness d requires an estimation of the oil specific attenuation coefficient α_o which must be derived from catalogs of optical signatures; in the data given in this paper, these values are measured with laboratory instrumentation from samples of the spilled mineral oils.

THE INSTRUMENT

In both experiments reported in this paper the Oceanographic Lidar System (OLS) developed at the University of Oldenburg was utilized. As the instrument has been previously described [Diebel-Langohr et al., 1985], only its most important specifications are given in Table 1.

Table 1 - Characteristics of the Oceanographic Lidar System (OLS).

excitation:		
lasers:	excimer	dye [1]
wavelength:	308 nm	450/533 nm
pulse length:	12 ns	6 ns
peak power:	10 MW	1 MW
rep. rate:	< 10 Hz [2]	
footprint at 200 m flight height:	2 m	0.5 m [3]
detection:		
telescope:	f/10 Schmidt-Cassegrain, diam. 0.4 m	
wavel. select.:	dichroic splitters, interference and blocking filters	
detection wavel.:	344-366-380-450/500-533-650-685-730 nm	
detectors:	PMT, EMI 9812, 9818	
digitizer:	Biomation 6500, 500 MHz, 6 bit	
system computer:	LSI 11/23 with floppy disk, magtape	

1) Only the excimer laser was utilised in ARCHIMEDES 2 and in the "MARPOL Exercise".

2) Signal repetition rate was 10 MHz in both experiments which corresponds to a footprint distance of 15 m in ARCHIMEDES 2 and 18 m in the "MARPOL Exercise".

3) Flight height was 700 ft in ARCHIMEDES 2 and 800 ft in the "MARPOL Exercise".

The sensor has been designed for applications in marine science aiming at a synoptic mapping of hydrographic conditions in extended coastal areas, which are rapidly changing in time, e.g. due to tidal currents and mixing. It is therefore a non-imaging sensor having excitation and detection wavelengths appropriate for the investigation of naturally occurring seawater compounds. Its main advantage lies in the capability of deriving depth profiles of hydrographic parameters in the water column when working in the time-resolving lidar mode [Diebel-Langohr et al., 1986]. The data reported in this paper were obtained by an off-line integration of time resolved signal returns, which is equivalent to a time-integrating fluorosensor mode.

As a result of the experience obtained in the experiment ARCHIMEDES 1 [Diebel-Langohr et al., 1985] the following modifications of the instrument were performed for a better operation over oil spills:

- only the excimer laser having an emission at 308 nm was utilized since dye laser operation at visible wavelengths does not result in signal returns that are very specific for the identification of mineral oil;
- for a closer spectral coverage of signal detection, the 500 nm detector wavelength (serving as the baseline for the 533 nm water Raman scatter measurement with 450 nm dye laser excitation) was shifted to 450 nm;
- an improved procedure for spectral calibration of the detection unit on the ground was developed making use of a 1 m^2 sheet of white teflon. The material has the advantage of possessing a fluorescence covering the near UV and visible spectrum when irradiated with the excimer laser, with an efficienty well corresponding to the typical water column and a mineral oil signal return. The spectral fluorescence emission of the teflon sheet is calibrated by comparison with a black body tungsten lamp;
- improved computer software allowed an increased continuous signal repetition rate of 10 Hz leading to a better footprint coverage;
- a photocamera was utilized under computer control and in parallel to the fluorosensor operation for a better identification of the flight path over the oil spills.

ARCHIMEDES 2

The experiment was conducted in the German Bight northwest of Helgoland on October 1-2, 1985. Operation of the Oceanographic Lidar System (OLS) installed in a Do 28 of DFVLR Oberpfaffenhofen was difficult due to bad weather conditions with very poor visibility at the operating altitude. Moreover, the Omega navigation system of the aircraft was defective on October 1. Since no long-range all weather guiding instrumentation was available onboard the aircraft, it was a matter of chance to find the position of oil spills. Due to this fact, only one of the three patches discharged, spill A, was found and investigated during sortie 2 on October 1.

Spill A, consisting of Ekofisk crude oil, was discharged on October 1, 6:30 - 6:40 hours, in a quantity of 1000 l. Spilling position was 54° 16.2' N, 7° 11,0' E. Ekofisk crude is a light mineral oil with low density of 0.874 and viscosity of 3.5 cst at 15°C [Schroh, 1986].

Four successful OLS overflights were made between 14:56 and 15:24 with various headings of the aircraft, see Table 2. As an example of the results, profiles obtained at different detection wavelengths are given as a function of the flight path in Fig. 1.

The film thickness distribution calculated from the depression of water Raman scatter intensity R according to the procedure discussed above is given in the same figure. For its evaluation, an attenuation coefficient $\alpha_o = c_1(308)+c_2(344) = 1\ \mu m^{-1}$ has been adopted according to the results of laboratory measurements with an absorption photometer; a 10% uncertainty of this measurement must be taken into account. Due to the fact that the optical characteristics of oil films on the water surface show rapid changes in time, the total relative error in the calculation of the film thickness is estimated to be about 30%.

Table 2 - Flights performed over spill A on October 2, 1985 (ARCHIMEDES 2).

TIME (loc)	FLIGHT NUMBER	HEADING	FIG.
14:56	042	280°	
15:12	044	310°	
15:20	046	170°	
15:24	047	160°	1-3

Fig. 2 shows a photograph taken during the same overflight, the flight path being given with a distance scale which corresponds to that of Fig. 1. The dark brown areas containing large amounts of oil correspond to OLS data with vanishing water Raman scatter intensity; two such spots are identified along the fluorosensor profile. Areas showing thin films with the typical silver colour, Fig. 2, are also found in the fluorosensor readings; their film thickness is typically 1 µm.

Closer inspection of the emission spectra reveals some interesting features. The clear water area outside the spill (at flight distances below 270 and above 600 m in Fig. 1) displays fluorescence originating from natural dissolved organic matter in the water column (Gelbstoff); in the 344 nm detection channel water Raman scatter also contributes to the intensity measured. Over the spill, signals from the water column are damped with increasing oil film thickness, and oil fluorescence is detected. The latter is low in the UV, but very dominant at green and red wavelengths.

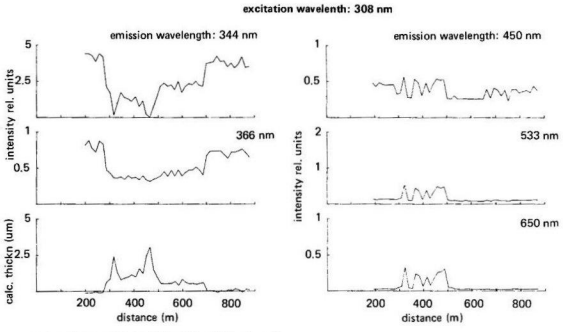

FIGURE 1 - OLS profile # 47 obtained over spill A on October 1, 1985, 15:24 h, heading 160°. Signals obtained at different wavelengths with 308 nm excitation are plotted as a function of the flight distance. Aircraft track over the spill is shown in Fig. 2 for comparison. The film thickness distribution displayed on the left below is calculated from the water Raman scatter intensity in the detection channel 344 nm after correction for fluorescence contributions at this emission wavelength by extrapolation of the 366 and 380 nm detection channels. At distances 315 and 460 m the upper limit of thickness measurements is exceeded, and no data are given.

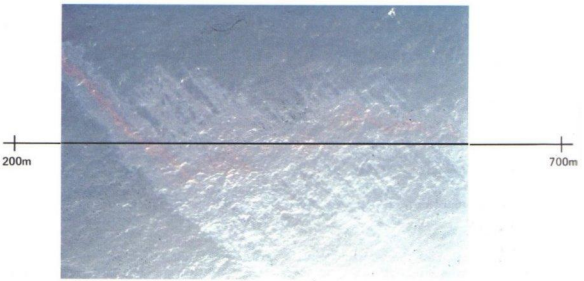

FIGURE 2 - Photograph of spill A taken during overflight # 47. The flight line and distance scale is indicated for comparison of the image with the fluorosensor data shown in Fig. 1.

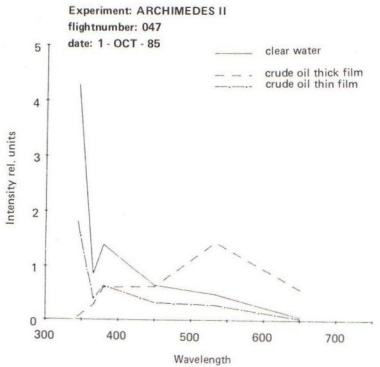

FIGURE 3 -Examples of emission spectra obtained from spill A and the surrounding oil-free water. Spectral position of detection channels is at 344, 366, 380, 450, 533 and 650 nm. Water Raman scatter is observed at 344 nm, the other detection wavelengths reflect fluorescence of the mineral oil and of Gelbstoff in the water column.

However, the change of the optical signature above the spill is not unambiguous:
- the 344 nm Raman channel shows very low intensity at the positions of the thick films; hence, the oil fluorescence is negligible at this wavelength; in the presence of thin films the intensity is about 50% of the clear water value, representing the damped water column signal;
- the 366 nm data are virtually constant over the spill and independent of the film thickness, also taking on about 50% of the clear water value; this signal is composed of oil fluorescence, and - above the thinner parts of the spill - of Gelbstoff fluorescence from the water column;
- the 450 nm channel shows again oil and Gelbstoff fluorescence, but the intensity over the thick parts of the spill is higher and that of the thin films lower, compared to the Gelbstoff fluorescence measured over clear water;
- at green and red wavelengths, corresponding to the 533 and 650 nm channels, Gelbstoff fluorescence is very low, but the high values of oil fluorescence are still comparable to those found in the UV and blue; no signal could be detected in the 730 nm channel.

The ambiguity at blue/green wavelengths which was also observed in the ARCHIMEDES 1 experiment, was explained by the fact that the oil used decomposed into fractions of different mechanical and optical characteristics due to the influence of wind and waves; with the heavy fuel used in ARCHIMEDES 1, this process can be easily observed in laboratory experiments [Diebel-Langohr et al., 1985]. Obviously, a similar effect is also found in ARCHIMEDES 2 with light crude oil.

THE MARPOL EXERCISE

In this experiment, a specific situation was prepared which is typically found in the case of controlled discharges of small volumes of mineral oil by ship traffic. In particular, it aimed at an investigation of the detection capabilities of remote sensors if a moving ship spills 60 liters of oil, or water containing 200 ppm of oil per nautical mile. These values correspond to the internationally accepted upper limits of permitted discharges near the coast line and in open sea areas.

The exercise was performed northwest of Rotterdam on May 7, 1986 in cooperation with Rijkswaterstaat.

Two oils were used for the 60 l/n.m. test:
- a mixture of gasoil, fuel, lubrification and crude oil originating from Cameroun (referred to as "crude" in the following), having a density of 0.850 and a viscosity of 8.44 cst at 20°C;
- light Diesel fuel with very low viscosity, having a good transparency with a light brown colour; no physical data are actually available for this oil.

Discharge was done from the oil combatting vessel "Smal Agt" of Rijkswaterstaat. An "Isowake" - type spill was produced several kilometers long and 10 - 50 m wide. For the 60 l/n.m. tests, this amount of oil was mixed with 100 m^3 of seawater before spilling. Absolute amounts of oil discharged during the 200 ppm test are not known.

Due to the good weather conditions during the experiment with clear sky and wind of about 4 bft, the 60 l/n.m. spills could be easily seen along the ship track, an example being given in Fig. 5. On the other hand, the 200 ppm discharge did not result in a visible surface film; according to information given by Rijkswaterstaat, this spill was not detectable with airborne SLAR and UV/IR scanner either [Schriel, 1986].

In this experiment, OLS was installed in the Do 228 research aircraft of DFVLR Oberpfaffenhofen. Several flights were made along the ship track, see Table 3, yielding a successful detection and analysis of the 60 l/n.m. oil spills . As with the airborne instruments used by Rijkswaterstaat, the 200 ppm spill could not be identified with the fluorosensor.

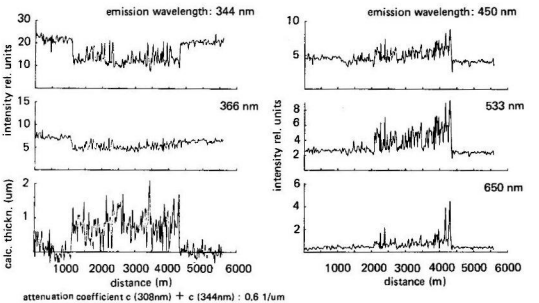

FIGURE 4 - OLS profile # 109 obtained over the 60 l/n.m. crude oil spill on May 7, 1986, 7:45 h. Signals obtained at different wavelengths with 308 nm excitation are plotted as a function of the flight distance. Ship position is at 4300 m in the distance scale. The film thickness distribution displayed on the left below is calculated from the water Raman scatter intensity in the detection channel 344 nm after correction of fluorescence contributions at this emission wavelength by extrapolation of the 366 and 380 nm detection channels.

Three examples of OLS profiles are shown in Figs. 4, 7 and 9:

- profile # 109, Fig. 4, was obtained over the crude oil film at 7:45 h. Start of spilling was 17 minutes earlier, corresponding to position 1100 m in the distance scale, Fig. 4, the ship being at position 4300 m during overflight;
- profile # 111 was obtained at 7:56 h, about 3 minutes after start of Diesel discharge at position 4600 m, the ship being at position 5700 m in Fig. 7;
- profile # 116 was measured at 8:25 h, the ship being at position 11000 m; discharge of Diesel had been stopped, and 200 ppm spillage was made at 8:17 at position 8000 m in Fig. 9.

According to the data shown in Fig. 4, the crude oil spill is clearly identified. The signal fluctuations observed over the spill area are not caused by electronic noise, but they result from the meandering shape of the spill due to wind stress on the sea surface. Therefore, about 20% of the footprints meet the clear water surface.

The intensity observed in the 344 nm water Raman scatter detection channel is depressed by about 50% in the presence of oil; this residual intensity is due to contributions originating from the water column, and to oil fluorescence, the latter being not negligible at this short emission wavelength due to the dominating light components of the oil type used. At blue, green and red emission wavelengths the fluorescence intensity received over oil is well above the clear water fluorescence values and increases significantly along the flight track in the direction of the spilling ship.

The film thickness displayed in Fig. 4 is derived from the depression of water Raman scatter as outlined previously, assuming that the sum of attenuation coefficients of the oil takes on a value of $c(308) + c(344) = 0.6\ \mu m^{-1}$. Thickness data of 1-2 μm obtained in this way are in the order of the values expected from the amount of spilled oil producing a plume about 20 m wide behind the ship.

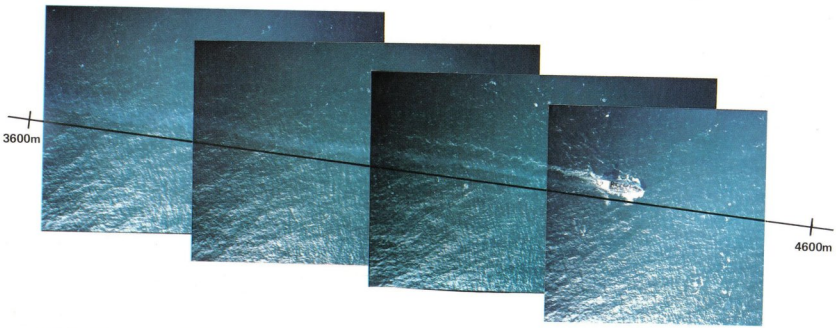

FIGURE 5 - Photographs of the 60 l/n.m. crude oil spill taken during overflight # 109. The distances given correspond to the scale of Fig. 4.

The data obtained in profile # 111, Fig. 7, describe the same crude oil spill, and the optical signature of the crude oil corresponds well to that observed in profile 109. However, the fluorescence signature of the light Diesel oil shows marked differences: fluorescence emission in the UV is very high, obscuring the water Raman scatter intensity in the 344 nm channel almost completely, and the fluorescence at green and red wavelengths is low resulting in intensities which do not significantly differ from those received over clear water.

Table 3 - Flights performed on May 7, 1986 (MARPOL Exercise).

TIME (loc)	LATITUDE START/END	LONGITUDE	FLIGHT NUMBER	SPILL CRUDE DIESEL/BILGE	FIG.
7:28		start spilling of crude oil, 60 l/n.m.			
7:39:20	52°15.9	4°10.4	108	c	
7:40:20	52°17.8	4°10.2			
7:44:24	52°15.1	4°10.6	109	c	4-6
7:46:13	52°18.3	4°10.2			
7:50:05	52°15.1	4°10.3	110	c	
7:51:39	52°18.2	4°10.3			
7:53		start spilling of Diesel oil, 60 l/n.m.			
7:55:36	52°15.4	4°10.5	111	c/d	7-8
7:57:20	52°17.0	4°10.4			
8:06:27	52°15.3	4°10.6	113	c/d	
8:08:55					
8:13:18	52°15.2	4°10.5	114	c/d	
8:15:47	52°20.7	4°10.9			
8:17		start spilling of bilge oil, 200 ppm			
8:25:00	52°14.9	4°10.2	116	c/d/b	9
8:28:22	52°22.2	4°09.6			
8:36:44			119	c/d/b	
8:38:52	52°23.1	4°09.2			

Thickness distribution of the crude and Diesel spill is again displayed in Fig. 8. For its calculation, an attenuation coefficient $c(308) + c(344) = 0.6\ \mu m^{-1}$ is tentatively chosen for both oil types.

Profile # 116, Fig. 9, shows the same situation about 30 minutes after the end of the crude oil spilling, and about 10 minutes after the end of the Diesel spilling. These data are quite remarkable since the characteristic optical signature of both oil types as measured in the preceding profiles (Figs. 4 and 7), disappeared completely. The dominating influence on the fluorosensor signal is in the near UV where a signal depression of 50% is found for both oil types. A similar but more moderate tendency is also observed at visible wavelengths.

Calculation of the film thickness from the water Raman scatter intensity yields again realistic values of about 0.5-1 µm for both oil types, Fig. 9. This is also supported by the fact that the spills could be well identified by visual observation during overflight. However, the components of the oils present within these spills during profile # 116 must be very different in their composition from the original ones.

The 200 ppm discharge which corresponds to positions 8000 - 11000 m in Fig. 9, does not result in a fluorosensor signal which can be distinguished from the data received over clear water. As already mentioned, this discharge did not give rise to a surface film that could be visually observed or identified by any other type of remote sensor.

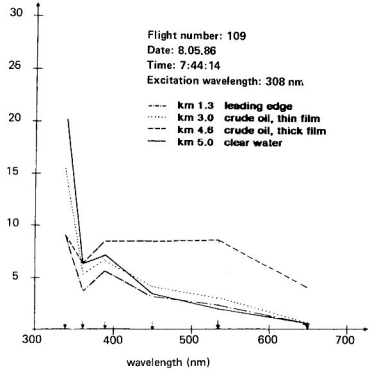

FIGURE 6 - Examples of emission spectra obtained from the 60 l/n.m. crude oil spill and the surrounding oil-free water, profile # 109. Spectral position of detection channels is indicated by arrows. See Fig. 4 for comparison.

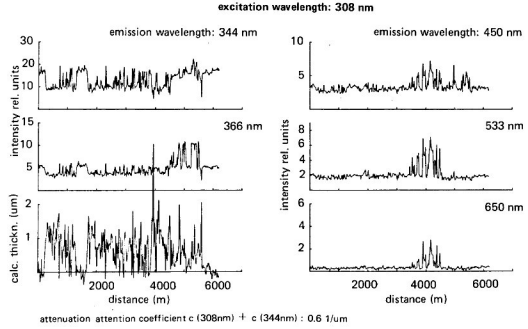

FIGURE 7 - OLS profile # 111 obtained over the 60 l/n.m. crude oil and Diesel spills on May 7, 1986, 7:55 h. Crude oil ends, and Diesel begins at position 4600 m. Ship position is at 5700 m.

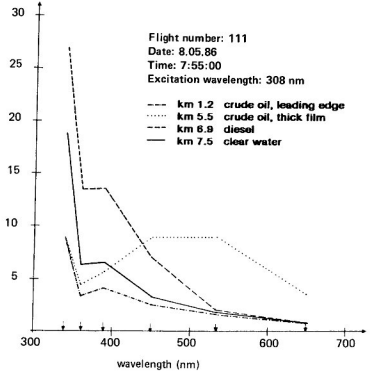

FIGURE 8 - Examples of emission spectra obtained from the 60 l/n.m. crude oil and Diesel spills and the surrounding oil-free water, profile # 111. Spectral position of detection channels is indicated by arrows. See Fig. 7 for comparison.

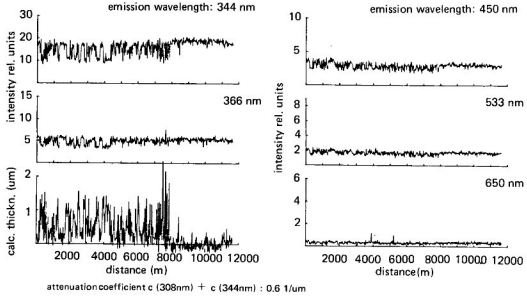

FIGURE 9 - OLS profile # 116 obtained over the 60 l/n.m. crude oil and Diesel spills and the 200 ppm spill on May 7, 1986, 8:25 h. Crude oil ends and Diesel begins at position 4500 m. Diesel ends and 200 ppm discharge begins at position 8000 m. Ship position is at 11000 m.

CONCLUSION

The capabilities of the airborne laser fluorosensor method for the investigation of small discharges of mineral oil has been well demonstrated in the experiments described in this paper. Even over coastal waters mostly exhibiting a strong fluorescence background due to large amounts of dissolved organic matter of natural origin, mineral oil can be easily identified and spectroscopically analyzed.

In particular, laser fluorosensor data reveal the following information:
- film thicknesses of surface layers can be obtained ranging from 0.1 to 10 μm;
- different mineral oils can be distinguished from their specific fluorescence signature.

However, some questions are still open and need further investigation. They mainly concern the changes in optical parameters of mineral oils in the case of surface films in the 1 μm thickness range.

It is found that these films alter their fluorescence properties completely within periods of 20 minutes after spilling. This statement holds even if the surface films do not show any modifications that can be observed by visual inspection. It is in particular found that those compounds responsible for the high fluorescence efficiency of oils disappear almost completely. This process can certainly be attributed to dissolution into the upper water layers and to evaporation into the atmosphere. This is obviously of lower relevance for compounds possessing low fluorescence efficiency.

On the other hand, data interpretation is mostly difficult for the results of the "MARPOL Exercise". It is not clear to which extent the utilized spilling procedure - i.e. the dispersion of the oil within large quantities of seawater before spilling - changes the optical properties of the oil, nor is it known what effects occur if after some time the oil dispersed in the upper water column floats to the water surface and produces surface films; this concerns both the properties of the oil itself and the consequences on the fluorosensor signal which is obtained by averaging over the 1 m footprint diameter.

The influence of the surface film on the sea surface roughness may also contribute to the signal change over the weathered oil film compared to the surrounding clear water. It is surprising to note that the observed depression of the signal intensity showing higher values at UV and blue wavelengths compared to the green and red spectral range was also found in the case of monomolecular films of oleyl alcohol which is a strong surface active material [Hühnerfuß et al., 1986]. It is not known if the signal depression observed in our experiments with oil films being thick compared to these monolayers is a consequence of the same optical mechanisms. Understanding and a quantitative explanation of this mechanism are still incomplete.

ACKNOWLEDGEMENTS

Development of the Oceanographic Lidar System OLS was financed by a grant from the Bundesministerium für Forschung und Technologie, Bonn. The experiments reported in this paper were supported by DFVLR Oberpfaffenhofen (FRG), Joint Research Centre Ispra of the EC Commission, by Rijkswaterstaat (The Netherlands), and by the Sonderstelle des Bundes "Ölunfälle See/Küste", Cuxhaven (FRG).

REFERENCES

Hoge F.E. and Swift R.N., 1980, Oil film thickness measurement using airborne laser-induced water Raman backscatter. Appl. Opt. 19: 3269-3281.

Hoge F.E., 1982, Laser measurement of the spectral extinction coefficients of fluorescent, highly absorbing liquids. Appl. Opt. 21: 1725-1729.

Hoge F.E., 1983, Oil film thickness using airborne laser-induced oil fluorescence backscatter. Appl. Opt. 22: 3316-3317.

Hoge F.E. and Swift R.N., 1983a, Airborne detection of oceanic turbidity cell structure using depth-resolved laser-induced water Raman backscatter. Appl. Opt. 22: 3778-3786.

Hoge F.E. and Swift R.N., 1983b, Experimental feasibility of the airborne measurement of absolute oil fluorescence spectral conversion efficiency. Appl. Opt. 22: 37-47.

Hühnerfuß H., Garett W.D. and Hoge F.E., 1986, The discrimination between crude oil spills and monomolecular sea slicks by an airborne lidar. Int. J. Remote Sensing 7: 137-150.

Kung R.T. and Itzkan I., 1975, Absolute oil fluorescence conversion efficiency. Appl. Opt. 15: 409-415.

O'Neil R.A., Buja-Bijunas L., and Rayener D.M., 1980, Field performance of a laser fluorosensor for the detection of oil spills. Appl. Opt. 19: 863-870.

Reuter R., Diebel-Langohr D., Dörre F. and Hengstermann T., 1986, The influence of Gelbstoff on remote sensing of seawater constituents from space. Appendix 9. Airborne laser fluorosensor measurements of Gelbstoff. ESA Contract No. RFQ 3-5060/84/NL/MD. GKSS Research Centre, 20 pp., in press.

Schriel R.H., 1986, Personal communication.

Schroh K., 1986, The logistics and local arrangements of the ARCHIMEDES 2 experience. Sonderstelle des Bundes "Ölunfälle See/Küste", internal report, 6 pp.

Schwarz J., 1982, Consolidation of NRC oil spectra onto single magnetic tape: NRCOIL. DAD Technical Note 1982-07, Canada Centre for Remote Sensing, Ottawa, Canada, 79 pp.

Thruston A.D. Jr. and Knight R.W., 1971, Characterization of crude and residual-type oils by fluorescence spectroscopy. Env. Sci. Tec. 5: 64-69.

Visser H., 1979, Teledetection of the thickness of oil films on polluted water based on the oil fluorescence properties. Appl. Opt. 18: 1746-1749.